THE JOURNAL OF BIOLOGICAL CHEMISTRY VOL. 282, NO. 21, pp. 15597–15605, May 25, 2007


# Kinetic and Structural Analysis of the Early Oxidation Products of Dopamine

## *ANALYSIS OF THE INTERACTIONS WITH α-SYNUCLEIN**

Received for publication, November 27, 2006, and in revised form, February 23, 2007 Published, JBC Papers in Press, March 29, 2007, DOI 10.1074/jbc.M610893200

**Marco Bisaglia[‡], Stefano Mammi[‡§1], and Luigi Bubacco[¶]**

*From the Departments of [‡]Chemical Sciences and [¶]Biology, University of Padova, and [§]Institute of Biomolecular Chemistry, Consiglio Nazionale delle Ricerche, I-35131 Padova, Italy*

**Oxidative stress appears to be directly involved in the pathogenesis of several neurodegenerative disorders, including Alzheimer and Parkinson diseases. Nigral dopaminergic neurons are particularly exposed to oxidative stress because a pathological accumulation of cytosolic dopamine gives rise to various toxic molecules, including free radicals and reactive quinones. These latter species can react with proteins preventing them from exerting their physiological functions. Among the possible targets of quinones, α-synuclein is of primary interest because of its direct involvement in dopamine metabolism. Contrary to the neurotoxic processes, neuromelanin synthesis seems to play a protective role by its ability to sequester a variety of potentially damaging substances. In this study, we carried out a kinetic and structural analysis of the early oxidation products of dopamine. Specifically, considering the potential high toxicity of aminochrome for both cells and mitochondria, we focused our attention on its rearrangement to 5,6-dihydroxyindole. After the spectroscopic characterization of the products derived from the oxidation of dopamine, the structural information obtained was used to analyze the reactivity of quinones toward α-synuclein. Our results suggest that indole-5,6-quinone, rather than dopamine-o-quinone or aminochrome, is the reactive species. We propose that the observed reactivity could represent a general reaction pathway whenever cysteinyl residues are absent in proteins or if they are sterically protected.**

Parkinson disease, the second most common neurodegenerative disorder, is a chronic and progressive disease characterized by degeneration of dopaminergic neuromelanin-containing neurons in the *substantia nigra pars compacta* (1) and by the presence of cytoplasmic inclusions that are mainly composed of fibrillar α-synuclein (αsyn)[2] (2). Postmortem studies support the involvement of oxidative stress and the production of reactive oxygen species in Parkinson disease (3, 4). A possible source of oxidative stress is the redox reactions that specifically involve dopamine (DA). A critical aspect is the amount of DA present in the cytoplasm, outside the synaptic vesicles where the neurotransmitter is confined under physiological conditions. Spontaneous oxidation of DA in the presence of molecular oxygen leads to the formation of several cytotoxic molecules, including superoxide anions ($O_2^{\cdot-}$), hydroxyl radicals ($OH^{\cdot}$), and reactive quinones (DAQs) (5). Reactive oxygen species derived from the oxidation of DA can damage cellular components such as lipids, proteins, and DNA (6). The electron-deficient quinones can also react with cellular nucleophiles, leading to further cytotoxicity. DAQs have been shown to bind covalently to cysteinyl residues of proteins both *in vitro* and *in vivo* (7–12). Because these residues are often located at the active site of a protein, it has been proposed that covalent modifications result in an impairment of protein function with potentially deleterious effects on the cell (10). Among the several proteins that appear to be physiological targets of DAQs, α-synuclein is of particular interest because it seems to be directly involved in DA storage, synthesis, and uptake (13). Therefore, modifications induced by DAQs on αsyn that prevent the protein from exerting its physiological function could generate a circular process that leads to an increased cytosolic DA concentration that in turn exacerbates the oxidative damage in dopaminergic neurons.

As a neurotransmitter, DA is synthesized in the cytoplasm and rapidly sequestered by the VMAT2 transporter into synaptic vesicles (14, 15) where it is stabilized by the low pH. When the amount of cytosolic DA exceeds the physiological concentration, DA can be metabolized via monoamine oxidase and aldehyde dehydrogenase into the non-toxic metabolite 3,4-dihydroxyphenylacetic acid and hydrogen peroxide (16) or it can be sequestered into the lysosomes (17) where it can auto-oxidize to form neuromelanin (NM). NM is a dark polymer present in the brain of humans and, to a lesser amount, of some other primates. It is primarily distributed in the dopaminergic neurons of the *substantia nigra* and the noradrenergic neurons of the *locus coeruleus* (18). No physiological function has been defined for NM, although the hypothesis of a protective role has been suggested in the literature. This role seems to be related to the ability of NM to sequester a variety of potentially damaging substances, such as toxic catechol derivatives, hydroxyl radicals, or redox active transition metals, including iron and copper (17, 19–21). The pathway for NM genesis, which involves DA oxidation, has been proposed to be similar to that originally

* This work was supported by a grant from the Italian Ministry of Education, University and Research (PRIN) and Fondo per gli Investimenti della Ricerca di Base. The costs of publication of this article were defrayed in part by the payment of page charges. This article must therefore be hereby marked "*advertisement*" in accordance with 18 U.S.C. Section 1734 solely to indicate this fact.

[1] To whom correspondence should be addressed: Dept. of Chemical Sciences, University of Padova, Via Marzolo, 1, I-35131 Padova, Italy. Tel.: 390498275293; Fax: 390498275239; E-mail: stefano.mammi@unipd.it.

[2] The abbreviations used are: αsyn, α-synuclein; AC, aminochrome; DA, dopamine; DAQs, dopamine-derived quinones; DHI, 5,6-dihydroxyindole; DQ, dopamine-3,4-quinone; IQ, indole-5,6-quinone; NM, neuromelanin.

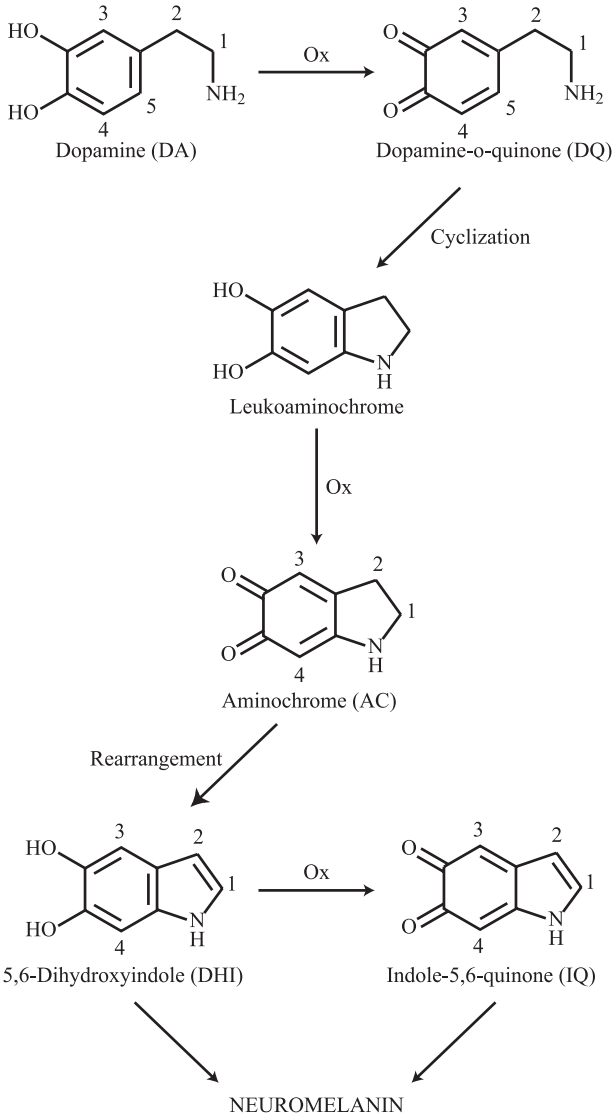


FIGURE 1. **The oxidative pathway of neuromelanin synthesis.** It is proposed by analogy with that described for the tyrosinase-mediated oxidation of dihydroxyphenylalanine (22, 23). The initial reaction involves the oxidation of dopamine (*DA*) to yield the corresponding dopamine-o-quinone (*DQ*). The two following steps are the cyclization of the quinone to give leukoaminochrome and its subsequent oxidation to aminochrome (*AC*). Then, aminochrome rearranges to 5,6-dihydroxyindole (*DHI*), which can be oxidized to indole-5,6-quinone (*IQ*) and polymerize to form neuromelanin. It is worth mentioning that in addition to the polymerization products described above, neuromelanin seems to include also uncharacterized proteinaceous and lipidic components as well as cysteinyl derivates (21). For each molecule, the protons observable in the NMR spectra are *numbered*.

described by Raper and later by Mason in their pioneering work on melanogenesis (22, 23). It is shown in Fig. 1. The overall process does not require enzymatic action (17, 21). However, tyrosinase, the trigger of melanin formation, has been recently detected in brain tissues (24).

Understanding the kinetics of the early steps in NM synthesis is important because of the potential neuroprotective role of neuromelanins. The goal is to determine the factors that prevent its formation, exposing the cell to damaging oxidative conditions. Until now, the kinetic information available in the literature has been primarily obtained for the first two steps of NM synthesis, *i.e.* dopamine-o-quinone (DQ) formation and its cyclization, or from studies carried out on dihydroxyphenylalanine (25–28). However, a different behavior was observed in the cyclization step using DA instead of dihydroxyphenylalanine (29), indicating, as expected, that the presence of the carboxyl group can influence the kinetics of the reactions.

In this study, we characterized the early oxidation products of dopamine by nuclear magnetic resonance. Specifically, considering the potentially high toxicity of aminochrome (AC) for both cell and mitochondria (30–32), we focused our attention on its rearrangement to 5,6-dihydroxyindole (DHI). Furthermore, by generating DA-derived quinones in a sample containing partially deuterated αsyn, we characterized the most reactive quinone demonstrating the potential reactivity of indole-5,6-quinone (IQ) toward αsyn.

## EXPERIMENTAL PROCEDURES

*Chemicals*—Dopamine hydrochloride, sodium (meta)periodate, sodium phosphate salts, and L-ascorbic acid were obtained from Sigma-Aldrich. Water-$d_2$ and sodium 3-trimethylsilyl propionate-2,2,3,3-$d_4$ were purchased from Cambridge Isotope Laboratories.

*Protein Preparation and Purification*—Human α-synuclein cDNA was subcloned into the NcoI and XhoI restriction sites of the pET28b plasmid (Novagen). The protein was expressed in *Escherichia coli* BL21(DE3) cells grown in M9 minimal medium, using 95% $D_2O$ when protein deuteration was desired. After boiling the cell homogenate for 15 min, the soluble fraction, containing αsyn, was treated with 50% ammonium sulfate. The pellet was then resuspended, dialyzed, loaded into a 6-ml Resource Q column (Amersham Biosciences), and eluted with a NaCl gradient.

*UV Spectroscopy*—Spectra were recorded on a personal computer-interfaced diode array Agilent 8453 UV-visible spectrophotometer. Optical measurements were performed at 25 and 37 °C using HELLMA quartz cell with Suprasil windows and an optical path length of 0.1 cm. Experiments were recorded with 30-s delays on 2-mM DA samples in water alone or in the presence of 20 mM phosphate buffer, pH 7.4, saturated with nitrogen, and with the addition of 2 mM $NaIO_4$. The wavelength range was 190–1100 nm. Millipore Milli-Q water was always used in the preparation of stock solutions to avoid metal-induced oxidative processes on DA.

*NMR Experiments*—Spectra were recorded on a Bruker Avance DMX600 spectrometer equipped with a gradient triple resonance probe. Stock solutions of the reagents were obtained by dissolving them in 99.9% $D_2O$. Samples were then prepared by mixing the stock solutions to obtain the desired final concentrations. Sodium 3-trimethylsilyl propionate-2,2,3,3-$d_4$ was used as an internal chemical shift reference. After the transfer into the NMR tube, and before the addition of the oxidant, the samples were fluxed with dry nitrogen gas for ~15 min to remove dissolved oxygen. Two-dimensional homonuclear experiments were used to assist the assignment of the peaks that appeared during the progress of the melanogenesis reaction. DQF-COSY spectra were acquired with gradient coherence selection (33, 34) and Clean-TOCSY spectra were recorded in the phase-sensitive manner using the TPPI method (35, 36) with 100 ms of mixing time. All two-dimensional exper-

iments were carried out by collecting 400 increments, each one consisting of 8 scans and 2048 data points. The spectral width was 6000 Hz in both dimensions. Prior to Fourier transformation, the time domain data were multiplied by shifted sine-bell functions in the F1 dimension and Gaussian functions in F2; zero filling to 4K × 1K real points was employed to increase the digital resolution.

*Kinetics Studies*—After recording the spectrum of DA alone, sodium periodate was added to the solution, and the reaction was followed by recording a series of one-dimensional spectra at 2–4-min intervals. An initial delay of ~4 min was necessary for thermal equilibration of the sample and for probe tuning and field shimming. Series of experiments were carried out by varying the pH (6.0–7.4), the temperature (15–37 °C), and the sodium periodate concentration (1–4 mM). The spectra were processed with GIFA (37), and the data were analyzed with Origin. The quantitative determination of the various compounds was carried out by integration of the corresponding peaks. The known concentration of dopamine before the reaction was used to determine concentrations from peak areas. The Levenberg-Marquardt $\chi^2$ minimization algorithm was used to fit the data.

*αSyn-DAQ Interactions*—The reactions were performed in a final volume of 25 μl, at 37 °C, in 20 mM phosphate buffer, pH 7.4, in the presence of 500 μM α-syn and 1 mM DA (containing 5 mCi of radioactive [$^{14}$C]DA). After the addition of 1 mM sodium periodate, aliquots (3 μl) were taken at 5, 10, 15, 30, 45, 60, 90, and 120 min and mixed with 22 μl of gel loading buffer containing 5 mM ascorbic acid. The reaction products were separated by 12% SDS-PAGE and detected by autoradiography. In parallel, a control was performed by incubating for 90 min αsyn and DA in the same experimental conditions but without sodium periodate.

*Characterization of the Reactive Oxidation Product of DA*—Stock solutions of the reagents were obtained by dissolving them in 99.9% $D_2O$. They were then mixed to obtain a 500-μM αsyn sample in 20 mM phosphate buffer, in the presence of 1 mM dopamine. After the acquisition of a reference one-dimensional NMR spectrum, $NaIO_4$ was added to the sample to a final concentration of 1 mM, and the reaction was followed for 2 h by recording a series of one-dimensional spectra at 37 °C at 2-min intervals. An initial delay of ~2 min was necessary for thermal equilibration of the sample and for probe tuning and field shimming. When deuterated αsyn was used, the reagent concentrations were the following: 250 μM αsyn, 250 μM dopamine, 500 μM $NaIO_4$, and spectra were recorded at 4-min intervals.

## RESULTS

*UV Studies*—The time evolution of the UV-visible spectrum of DA in the presence of $NaIO_4$ is shown in Fig. 2. The reaction was first carried out in $H_2O$ without buffer, as described in a previous study (18). Upon addition of $NaIO_4$, the absorption at λ = 280 nm decreases, indicating the disappearance of dopamine. Immediately, an absorption maximum appears at λ = 395 nm, corresponding to the yellow chromophore DQ, which is progressively replaced by the orange AC (Fig. 2*A*). Two new features appear in the spectra at 300 and 475 nm that have been associated with AC (18). Under more physiological conditions, *i.e.* at 37 °C and pH 7.4, addition of the oxidant causes only the peaks corresponding to AC to arise while peaks relative to other intermediate species, and in particular to DQ, are not detected (Fig. 2*B*). The time evolution of AC can be easily followed; unfortunately, the quantitative analysis of the decay is hampered by the formation of a black precipitate that induces light scattering.

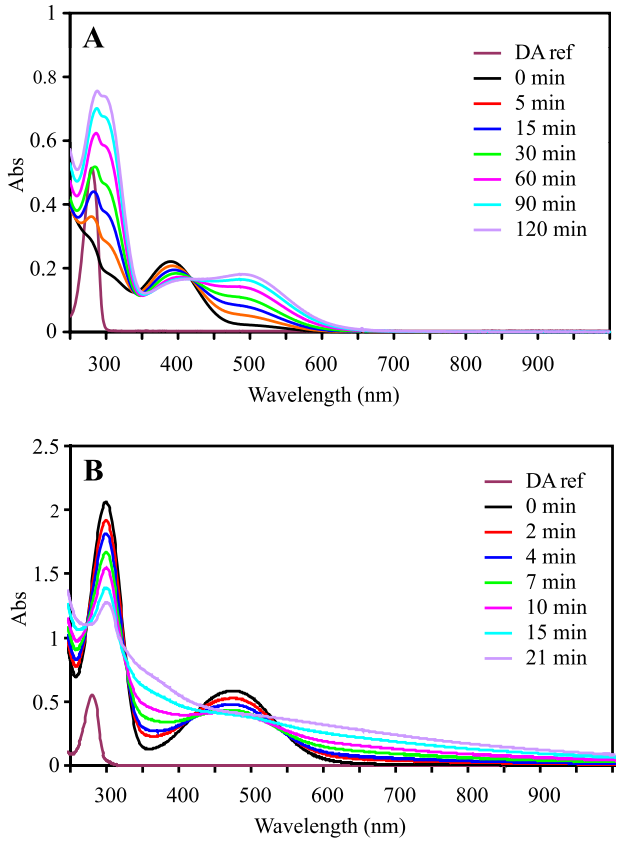


FIGURE 2. **The early steps of the oxidative pathway of neuromelanin formation analyzed by optical spectroscopy.** UV-visible spectrum of dopamine oxidation products after the addition of an equimolar amount of $NaIO_4$, recorded on a 2-mM DA sample in water (*A*) and in phosphate buffer (*B*) at pH 7.4. The peaks corresponding to aminochrome are easily visible in the spectrum. The black precipitate that appears as the reaction in phosphate buffer proceeds results in severe light scattering that hampers a quantitative analysis.

*NMR Assignment*—Before carrying out a kinetic analysis by NMR spectroscopy, it is mandatory to unambiguously assign each resonance observed in the spectra during the evolution of the polymerization process. In the present case, the transient character of many products complicated the assignment. However, by following the reaction at 25 °C in an unbuffered equimolar solution of DA and $NaIO_4$, the species DA, DQ, and AC were stable for enough time to record two-dimensional COSY and TOCSY experiments. The multiplicity of the peaks and chemical shift information available in the literature were also used for the assignment (38). In agreement with the UV analysis, when the NMR experiments were repeated at 37 °C, pH 7.4, a closer approximation of the physiological conditions, the formation of DQ was not detected. On the contrary, four new peaks appeared, two singlets and two doublets, later assigned to DHI. The one-dimensional spectrum recorded 10 min after the addition of the oxidant in these latter experimental conditions is shown in Fig. 3. All the NMR data obtained from our analysis are summarized in Table 1.

*Kinetics Studies*—After the assignment of the individual resonances, kinetics measurements were carried out at different concentrations of the oxidizing agent by acquiring series of one-dimensional spectra. Under the experimental conditions used, *i.e.* 37 °C, pH 7.4, a 2-mM DA solution was stable over several hours, excluding the contribution of autooxidative processes. To exclude possible interference by sodium 3-trimethylsilyl propionate-2,2,3,3-$d_4$ or transition metal ions, the experiments were repeated both without sodium 3-trimethylsilyl propionate-2,2,3,3-$d_4$ and in the presence of 2 mM EDTA with no observable differences.

Finally, to test whether radical species are formed in the early steps of the process (which should alter the peak intensities), we recorded a series of one-dimensional spectra in the presence of 2 mM phenylalanine as well as DA. After the addition of 2 mM $NaIO_4$ and the subsequent formation of AC and DHI, the peak intensities corresponding to phenylalanine were unchanged, indicating that even if the oxidizing process proceeds through formation of radicals, these do not affect peak intensities.

The pseudo-two-dimensional spectrum recorded at 37 °C, pH 7.4 in the presence of 2 mM DA after the addition of 1 equivalent of oxidant is shown in Fig. 4. All peaks relative to DA, AC, and DHI are visible, and the evolution can be followed over time. Under these experimental conditions and in the reaction

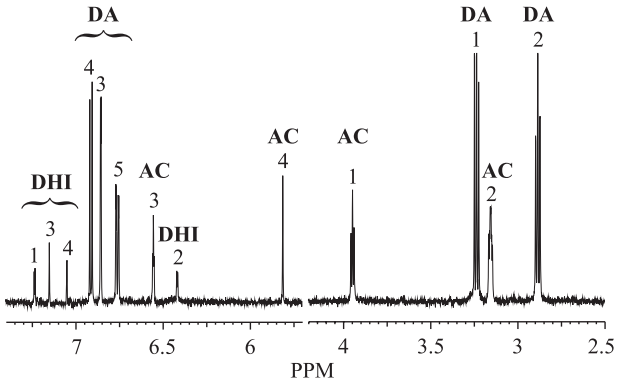


FIGURE 3. **NMR spectrum of the species observable during the early steps of the oxidative pathway of neuromelanin synthesis.** The spectrum was recorded at 37 °C, pH 7.4, on a 2-mM DA sample 10 min after the addition of an equimolar amount of $NaIO_4$. The resonance assignment is indicated on the spectrum using the notation of Fig. 1.

**TABLE 1**

**$^1$H NMR data and structural assignment**

s, singlet; d, doublet; t, triplet; dd, doublet of doublets; dt, doublet of triplets.

| Dopamine | | | Dopamine-o-quinone | | | Aminochrome | | | 5,6-Dihydroxyindole | | |
|---|---|---|---|---|---|---|---|---|---|---|---|
| δ | $^3J$ (H,H) | Assignment[a] | δ | $^3J$ (H,H) | Assignment[a] | δ | $^3J$ (H,H) | Assignment[a] | δ | $^3J$ (H,H) | Assignment[a] |
| *ppm* | *Hz* | | *ppm* | *Hz* | | *ppm* | *Hz* | | *ppm* | *Hz* | |
| 6.91 | d (8.1) | 4 | 7.14 | dd (10.2, 2.2) | 4 | 6.55 | t (2.6) | 3 | 7.23 | d (3.1) | 1 |
| 6.85 | d (2.1) | 3 | 6.49 | d (10.3) | 5 | 5.81 | s | 4 | 7.15 | s | 3 |
| 6.76 | dd (8.1, 2.2) | 5 | 6.38 | d (1.8) | 3 | 3.95 | t (5.3) | 1 | 7.05 | s | 4 |
| 3.23 | t (7.3) | 1 | 3.32 | t (7.5) | 1 | 3.15 | dt (2.6, 5.2) | 2 | 6.42 | d (3.0) | 2 |
| 2.88 | t (7.3) | 2 | 2.85 | t (7.5) | 2 | | | | | | |

[a] The notation is the same as in Fig. 1.

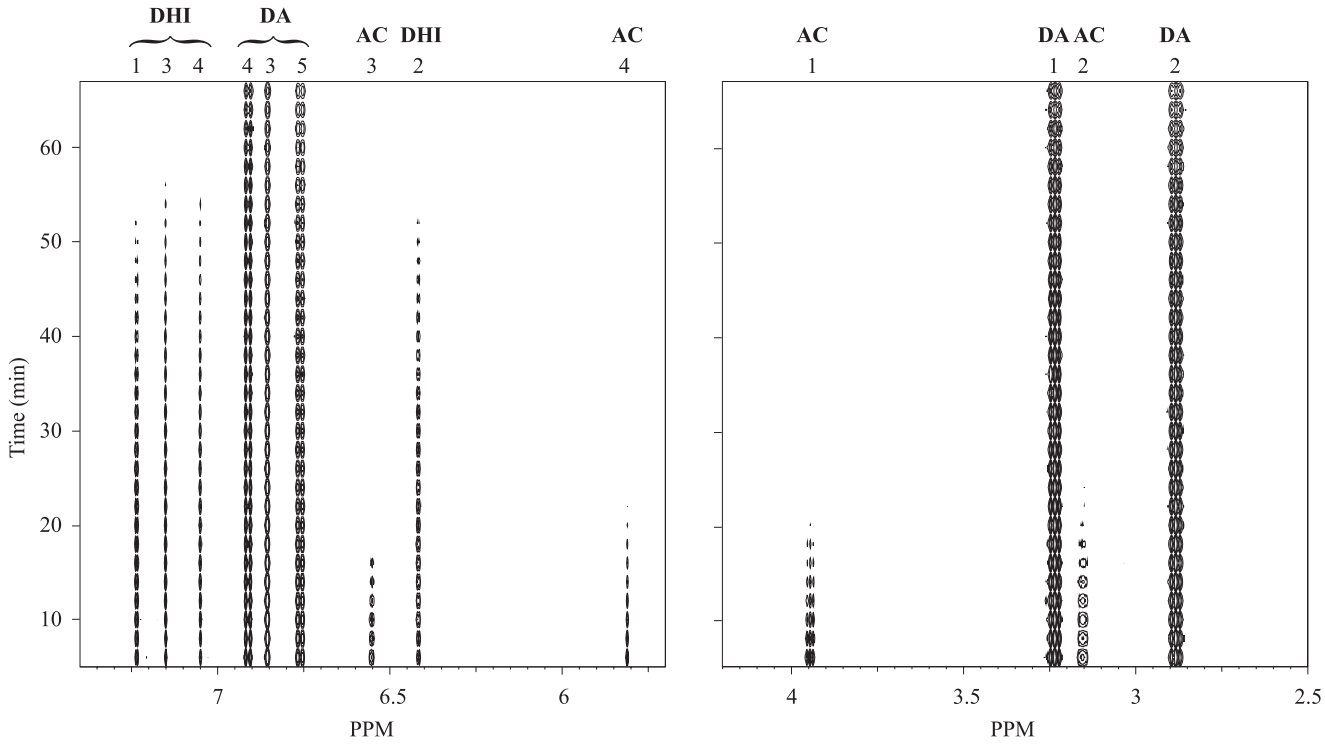


FIGURE 4. **The early steps of the oxidative pathway of neuromelanin formation analyzed by NMR spectroscopy.** A series of one-dimensional spectra was acquired at 37 °C, pH 7.4, on a 2-mM DA sample after the addition of an equimolar amount of $NaIO_4$. The time evolution of the peaks corresponding to dopamine, aminochrome, and 5,6-dihydroxyindole can be easily followed independently. The resonance assignment is indicated on the spectrum using the notation of Fig. 1.

time indicated, no peaks corresponding to oligomeric species appear. This result may be explained as follows: either the polymerization is too fast to allow the accumulation of dimers, trimers, and oligomers in high enough concentrations to be detectable by NMR, or the solubility of these species is below the NMR detection level, or a combination of the two.

For a quantitative analysis of the kinetics data, the concentrations of the different molecules were obtained from the integration of the corresponding peaks; the known initial concentration of DA (and of phenylalanine as an internal standard, when present) was used to determine concentrations from peak areas. The time evolution of DA, AC, and DHI at 37 °C, pH 7.4, starting from 2 mM DA in the presence of 1 equivalent of oxidant is shown in Fig. 5*A*. As expected, cyclization of DQ is very fast at pH 7.4 (27) so that $NaIO_4$ is consumed to oxidize not only DA, but also leukoaminochrome. Accordingly, a few seconds after the addition of the oxidant, DA and AC are present in solution approximately at the same concentration. The slow disappearance of DA, which continues for more than 1 h after the beginning of the reaction, may indicate that slight oxidative conditions are still present in solution. This may also justify the disappearance of DHI after its accumulation. Another possibility is that DA is partially sequestered during the formation of a precipitate that was always observed in the experimental conditions used in this work.

The overall reaction we studied can be summarized as follows,

$$\mathrm{DA} \xrightarrow[k_1]{} \mathrm{AC} \xrightarrow[k_a]{} \mathrm{DHI} \xrightarrow[k_b]{} \mathrm{IQ} \xrightarrow[k_2]{} \mathrm{Precipitate}$$

REACTION 1

where $k_1$ and $k_2$ are too fast to be followed by NMR (28) and $k_a$ and $k_b$ represent the apparent constants of the disappearance processes of AC and DHI, respectively.

The rearrangement of AC, which should not be affected by any oxidative condition, follows a first order kinetics curve, and the data can be fitted well (correlation factor >0.98) by Equation 1, $[AC] = [AC]_0 \exp\{-k_a t\}$, where [AC] is the aminochrome concentration, $[AC]_0$ is the concentration at time 0, *i.e.* a few seconds after the addition of $NaIO_4$, $t$ is time, and $k_a$ is the rate constant of the rearrangement reaction. The interpolation of the experimental data with Equation 1 leads to a value of $k_a = 0.16 \pm 0.02\ \mathrm{min}^{-1}$, where the error is the maximum deviation calculated on three separate experiments. In the simplest case of two consecutive first order reactions, we also calculated a value of $k_b = 0.073 \pm 0.018\ \mathrm{min}^{-1}$, where the uncertainty is the maximum deviation calculated on three separate experiments. This value of $k_b$, however, does not lead to a good fit of the time dependence of the variation in DHI concentration, suggesting that the observed consumption of DHI depends on more than one process, possibly of an order higher than one.

To verify the independence of the decay of AC from the presence of oxidant, different experiments were conducted varying the $NaIO_4$ concentration while keeping the initial DA concentration constant. As expected, the concentrations of DA and AC, a few seconds after addition of $NaIO_4$, were sensitive to the oxidant concentration (Fig. 5, *A–D*). On the

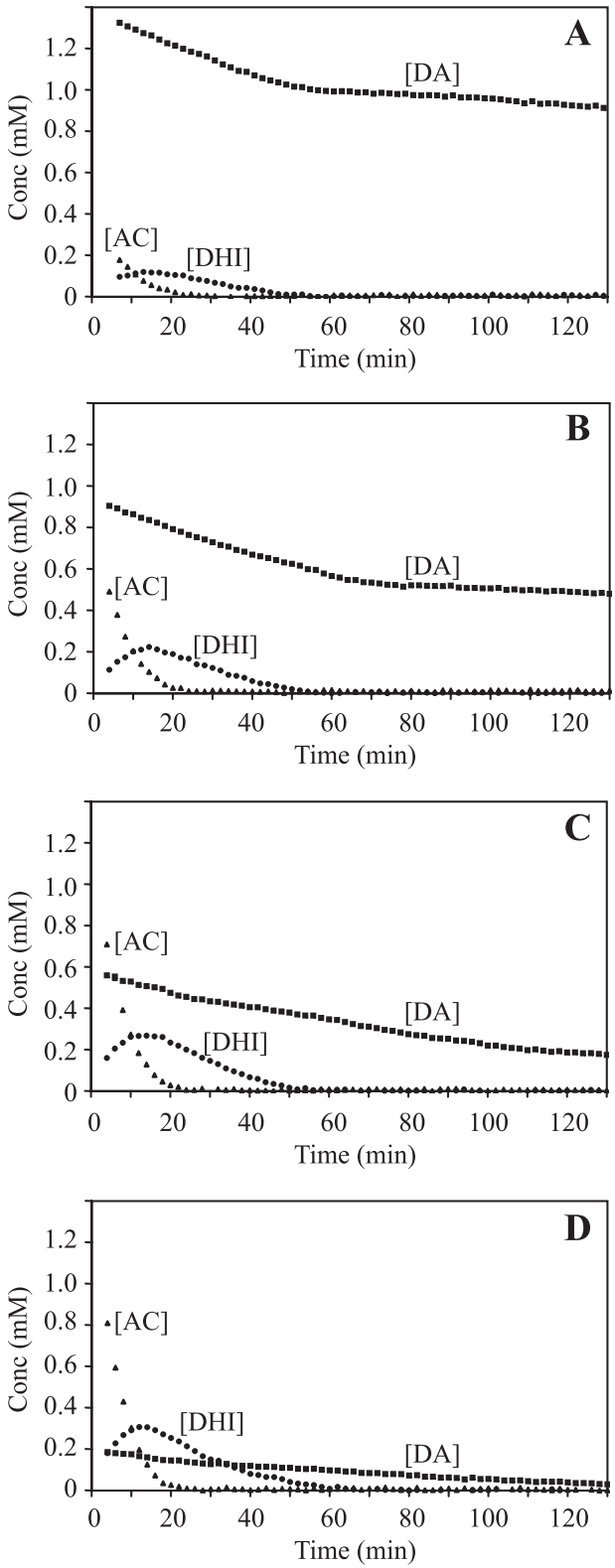


FIGURE 5. **Effects of different oxidant-to-DA ratios on the rate constant of aminochrome disappearance.** The plots represent the time evolution of DA, AC, and DHI, starting from 2-mM DA after the addition of various amounts of $NaIO_4$: 1 mM (*A*), 2 mM (*B*), 3 mM (*C*), 4 mM (*D*). The formation of a black precipitate is responsible for the eventual disappearance of the species observable by NMR.

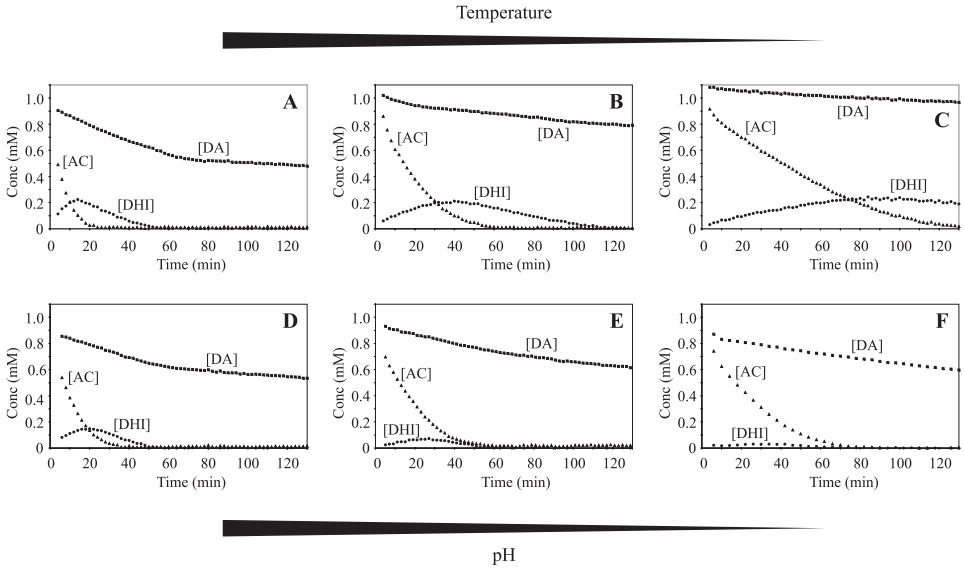


FIGURE 6. **Effect of temperature and pH on the rate constant of aminochrome disappearance.** The plots represent the time evolution of DA, AC, and DHI, starting from 2 mM DA after the addition of an equivalent amount of $NaIO_4$. The experimental conditions are the following: 37 °C, pH 7.4 (*A*); 25 °C, pH 7.4 (*B*); 15 °C, pH 7.4 (*C*); 37 °C, pH 7.0 (*D*); 37 °C, pH 6.5 (*E*); 37 °C, pH 6.0 (*F*). The formation of a black precipitate is responsible for the eventual disappearance of the species observable by NMR.

**TABLE 2**
**Effect of temperature and pH on the apparent rate constant for AC disappearance**

| | | | |
|---|---|---|---|
| $T$ (°C) (pH 7.4) | 37 | 25 | 15 |
| $k_a$ ($min^{-1}$) | 0.16 | 0.06 | 0.02 |
| pH ($T$ 37 °C) | 7.0 | 6.5 | 6.0 |
| $k_a$ ($min^{-1}$) | 0.10 | 0.06 | 0.04 |

contrary, the rate of disappearance of AC was not affected, and the kinetic constants found at oxidant-to-DA ratios of 1:2, 1.5:1, and 2:1 (0.16 ± 0.02, 0.18 ± 0.04, and 0.18 ± 0.03 $min^{-1}$, respectively) were consistent with the value found at a 1:1 ratio.

We also analyzed the effects of temperature and pH on the reaction rate (Fig. 6, *A–C*). Lowering the temperature causes a decrease of the rearrangement rate, as well as of all the reactions observed. Using the three points available, we estimated the value of the activation energy of the rearrangement reaction from the temperature dependence of its rate constant. The logarithmic plot of $k_a$ *versus* 1/T (data not shown) is a straight line (correlation factor >0.999), suggesting that the process follows Arrhenius's law as shown in Equation 2, $k_a = A \exp\{-E_a/k_B N_a T\}$, where the pre-exponential factor $A$ is a measure of the collision rate, $k_B$ is the Boltzmann constant, $N_a$ is Avogadro's number, $T$ is the temperature, and $E_a$ is the energy of activation. The linearity of the plot indicates that $E_a$ is independent of temperature. The interpolation of the experimental data leads to a value of $A = 7.28 \times 10^{10}$ $min^{-1}$ and $E_a = 69$ kJ $mol^{-1}$.

The kinetic constant decreases also with a decrease in pH, as shown in Fig. 6, *D–F*. However, the influence of pH seems to be more relevant for the rearrangement reaction. The accumulation of DHI at lower pH values is very limited, indicating that the rate of disappearance of DHI is much less affected by pH variations than the accumulation rate. The values of the calculated rate constants are summarized in Table 2.

*NMR Characterization of DAQ Species Reactive toward αSyn*—The spectroscopic characterization of all the species involved in the early steps of the NM synthesis allowed us to study their reactivity toward target proteins. Previous studies pointed to αsyn as a cytoplasmatic target for DAQs, suggesting a potential pathological effect of DAQ-modified αsyn. On these premises, we chose to characterize the most reactive DAQs toward this protein. DA reactivity has generally been ascribed to DQ, but αsyn lacks sulfhydryl groups. The latter are the nucleophilic groups in proteins that are usually reported to interact with DQ (7–12). Consequently, the reactive quinone species that are likely to be involved in the interaction with αsyn could be other ones. As indicated in Fig. 1, the quinones generated during the oxidative pathway of NM synthesis are DQ, AC, and IQ. Consequently, all of these are possible reactive species. To verify that DAQs react covalently with αsyn, the reaction with [$^{14}$C]DA was followed in time and the products identified by autoradiography of the SDS-PAGE. As shown in Fig. 7, immediately after the addition of the oxidant, a band corresponding to the αsyn monomer became visible, indicating the incorporation of the radioactive molecule into the protein. We observed other bands in the gel corresponding to dimeric and oligomeric forms of DAQ-modified αsyn. The relative intensities of these bands seemed to increase with increasing reaction time. Once the interaction of DAQs with αsyn was shown to lead to a covalent adduct, the monomeric species was characterized by NMR spectroscopy. The experiments were conducted in $D_2O$ to simplify the aromatic region of the spectrum. To exclude any possible interference of aspecific chemical modifications induced on αsyn by the oxidant, we followed the time evolution of the protein peaks in the presence of one equivalent of $NaIO_4$ in a control experiment. After an incubation delay of 1 h, no peak variation was observed. At first, the experiment was carried out using totally protonated αsyn. However, to make the analysis more informative, we repeated it with a partially deuterated sample of αsyn. This strategy allowed us to observe the peaks relative to DA-derived species more easily despite their low concentration and still follow the NMR signals of the protein. In Fig. 8, the one-dimensional spectra of partially deuterated αsyn and DA before and after the addition of $NaIO_4$ are shown. Peaks corresponding to DA were strongly reduced after the addition of the oxidant. Simultaneously, two new peaks became visible that were unambiguously assigned to AC on the basis of our previous assignment. The intensity of these peaks decreases with time while new peaks, relative to DHI, appear. The formation of DHI indicates that the earlier quinone species, *i.e.* DQ and AC, are not reactive enough toward the nucleophilic groups present in synuclein. A

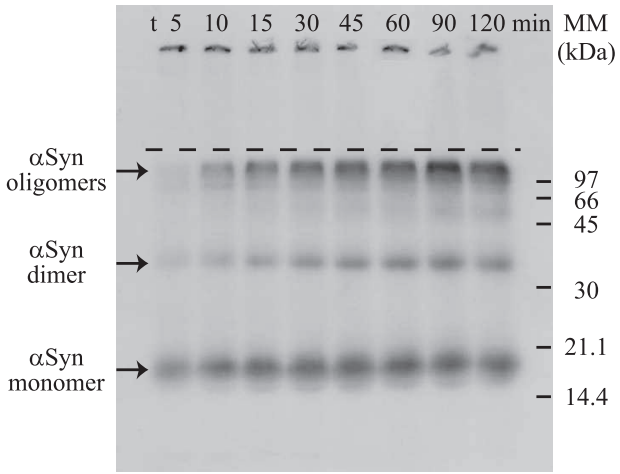


FIGURE 7. **Analysis of the interactions between α-synuclein and dopamine-derived quinones.** αSyn and [$^{14}$C]DA were incubated at 37 °C in the presence of $NaIO_4$, and aliquots were taken at different incubation times. Bands corresponding to αsyn monomeric, dimeric, and oligomeric species are visible in the gel, indicating the incorporation of the radioactive molecule in the protein. The *dashed line* represents the separation between stacking and resolving layers of the polyacrylamide gel.

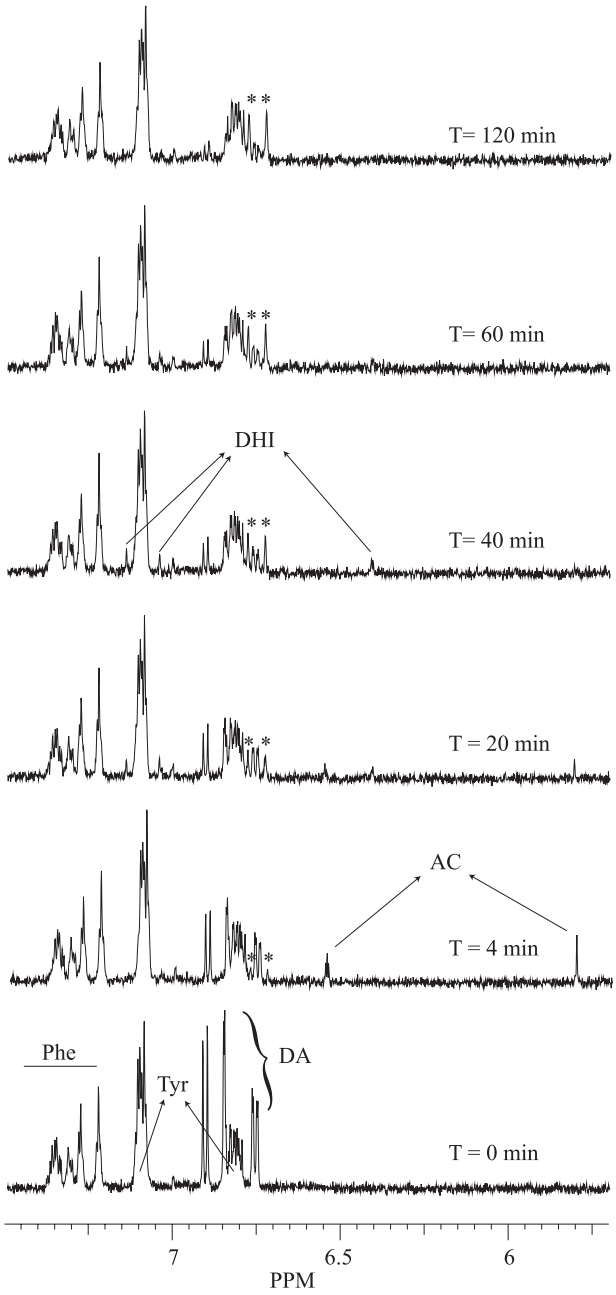


FIGURE 8. **Characterization of the most reactive dopamine-derived quinone.** The time evolution of the early oxidation products of DA were followed by a series of one-dimensional spectra acquired at 37 °C on a DA sample in the presence of partially deuterated αsyn after the addition of $NaIO_4$. The peaks corresponding to the previously characterized DA-derived species are visible during the evolution of the reaction. *Asterisks* indicate peaks that are tentatively attributed to a stable αsyn/DAQ adduct (see "Results").

hypothetical interaction of DQ and/or AC with αsyn would have produced new peaks in the NMR spectra, as shown in a previous work where the investigators used *N*-acetylcysteine as nucleophilic agent (39). The absence of such new peaks indicates that, if present, these products are below the detection threshold. In the experimental conditions presented here, we calculated this threshold to be between 10–15 μM. This means that a parallel reactivity of DQ and AC toward αsyn, which we cannot completely exclude, encompasses at the most 5% of the full DA reactivity. Therefore, we conclude that IQ is the first DA-derived quinone to react with αsyn in measurable amounts. In agreement with this conclusion is the appearance, a few minutes after the addition of the oxidant agent, of two singlets at 6.73 and 6.78 ppm (indicated by *asterisks* in Fig. 8). The growth profile of the intensity of these peaks is parallel to the profile of DHI decrease, and it reaches a plateau when the disappearance of DHI is complete, after ~70 min (data not shown). Although the characterization of these peaks remains elusive with the structural techniques at our disposal, this kinetic profile strongly indicates the formation of a stable αsyn/DAQ adduct, which we suggest to arise from the reaction of αsyn with IQ or one of its oligomeric derivatives.

## DISCUSSION

The level of cytosolic dopamine is maintained by feedback inhibition of tyrosine hydroxylase, mitochondrial monoamine oxidase, and dopamine transporter and by vesicular monoamine transporter 2-mediated accumulation into synaptic vesicles (17, 40). Neuromelanin has been suggested to act as an additional mechanism to regulate cytosolic DA by sequestering DA or its adducts in autophagic vacuoles/lysosomes (17, 19–21). A misregulation in the metabolism of dopamine or a defect in its compartmentation within the cell can lead to an increased concentration of this substance in the cytoplasm. As a consequence, dopamine may undergo auto-oxidation, giving rise to species that are potentially toxic for the cell, such as free radicals and quinones (dopamine-o-quinone, aminochrome, indole-5,6-quinone). Actually, oxidation products of DA have been shown to covalently bind to the sulfhydryl groups of proteins both *in vivo* and *in vitro* (7–12). Moreover, aminochromes formed after oxidation of dopamine, adrenaline, and noradrenaline have been shown to be reversible inhibitors of human brain dihydropteridine reductase (41, 42).

In this study, we first focused our attention on the kinetic characterization of the AC rearrangement at different temperatures and pH values. This is a fundamental step of neuromela-

nin synthesis and could be important in the DA-related oxidative stress within dopaminergic neurons.

The kinetic investigation of the rearrangement reaction is complicated by the fact that many processes occur simultaneously, as shown in Fig. 1. As a consequence, the relative concentration of each species, at a given point in time, is the result of several reactions. The system can be simplified using an oxidizing agent in which AC can be instantaneously produced from DA. Because the oxidizing agent does not affect the rearrangement of AC, the disappearance of the latter can be easily studied. As suggested by Graham and Jeffs (43), we chose to work with sodium periodate instead of other oxidants such as $Ag_2O$ and $H_2O_2$/peroxidase, because these proceed via free radical intermediates that would have hampered the NMR analysis and are less specific.

A considerable advantage of the NMR approach proposed here, relative to other spectroscopic techniques, is the possibility to observe the time evolution of the different species independently, without isolation steps. So, for the first time, the early steps of the complex oxidative process that leads to the formation of neuromelanin were analyzed by NMR.

After the structural characterization of the molecules involved in these reactions, we analyzed the reactivity of the DA-derived quinones toward α-synuclein. Actually, the DAQ reactivity observed, both *in vitro* and *in vivo*, toward the sulfhydryl groups of proteins has been ascribed to DQ (7–12). However, αsyn does not contain cysteine. Furthermore, at physiological pH, under pseudo-first order rate conditions where nucleophiles are present in excess, it has been shown that the reaction of most amino acids with dopamine-o-quinone is too slow to compete with its intramolecular cyclization (29). Two recent reports have described a reversible inhibition of αsyn fibril formation *in vitro* by aminochrome (44, 45), even if, in the incubation experiments described in those works, aminochrome could further evolve to generate the species described in Fig. 1. Because those observations suggest a possible involvement of AC in the interactions with αsyn, we decided to verify this hypothesis. By limited deuteration, the protein was made partially silent to the NMR, and we were able to follow the time evolution of the NMR signals corresponding to DA and its derived DAQs. The formation of AC was in fact observed, but the ensuing rearrangement reaction seems to be favored even when αsyn is present. Therefore, our analyses indicate that IQ, rather than DQ or AC, are the most reactive quinone species. We suggest that the reactivity observed for IQ could represent a general reaction pathway whenever cysteinyl residues are absent or when they are sterically protected.

Interestingly, the presence of αsyn in our incubation experiments stopped the polymerization process of DA. Under the experimental conditions used in this work, we never observed the presence of a precipitate, contrary to what happened incubating DA alone. This behavior is not generally observed when DAQs are generated in the presence of proteins. Enzymatic oxidation of DA in the presence of bovine serum albumin has been reported to give rise to a black, protease-resistant insoluble material (46). Although our experimental conditions are not an accurate representation of the cellular environment, this observation may provide an insight on the pathogenesis and/or the evolution of Parkinson disease, especially considering the potential neuroprotective role suggested for NM (17, 19, 20). More speculatively, if NM formation is prevented, then the redox active transition metals and other toxic molecules, generally captured within the NM structure, may become available in the cell, promoting or exacerbating oxidative conditions that can lead to cellular death. Although this hypothesis needs to be verified *in vivo*, the interplay between αsyn and NM deserves further consideration.

*Acknowledgment—We thank Dr. Michele Scian for critical review of this manuscript.*

## REFERENCES


1. Hirsch, E., Graybiel, A. M., and Agid, Y. A. (1988) *Nature* **334,** 345–348
2. Spillantini, M. G., Schmidt, M. L., Lee, V. M., Trojanowski, J. Q., Jakes, R., and Goedert, M. (1997) *Nature* **388,** 839–840
3. Hirsch, E. C. (1993) *Eur. Neurol.* **33,** Suppl. 1, 52–59
4. Jenner, P. (1998) *Movement Disorders* **13,** Suppl. 1, 24–34
5. Graham, D. G. (1978) *Mol. Pharmacol.* **14,** 633–643
6. Lotharius, J., and Brundin, P. (2002) *Nat. Rev. Neurosci.* **3,** 932–942
7. Ito, S., Kato, T., and Fujita, K. (1988) *Biochem. Pharmacol.* **37,** 1707–1710
8. Hastings, T. G., Lewis, D. A., and Zigmond, M. J. (1996) *Proc. Natl. Acad. Sci. U. S. A.* **93,** 1956–1961
9. Kuhn, D. M., Arthur, R. E., Jr., Thomas, D. M., and Elferink, L. A. (1999) *J. Neurochem.* **73,** 1309–1317
10. LaVoie, M. J., and Hastings, T. G. (1999) *J. Neurosci.* **19,** 1484–1491
11. Whitehead, R. E., Ferrer, J. V., Javitch, J. A., and Justice, J. B. (2001) *J. Neurochem.* **76,** 1242–1251
12. LaVoie, M. J., Ostaszewski, B. L., Weihofen, A., Schlossmacher, M. G., and Selkoe, D. J. (2005) *Nat. Med.* **11,** 1214–1221
13. Sidhu, A., Wersinger, C., and Vernier, P. (2004) *FASEB J.* **18,** 637–647
14. Erickson, J. D., Eiden, L. E., and Hoffman, B. J. (1992) *Proc. Natl. Acad. Sci. U. S. A.* **89,** 10993–10997
15. Liu, Y., Peter, D., Roghani, A., Schuldiner, S., Prive, G. G., Eisenberg, D., Brecha, N., and Edwards R. H. (1992) *Cell* **70,** 539–551
16. Elsworth, J. D., and Roth, R. H. (1997) *Exp. Neurol.* **144,** 4–9
17. Sulzer, D., and Zecca, L. (2000) *Neurotox. Res.* **1,** 181–195
18. Graham, D. G. (1979) *Arch. Pathol. Lab. Med.* **103,** 359–362
19. Sulzer, D., Bogulavsky, J., Larsen, K. E., Behr, G., Karatekin, E., Kleinman, M. H., Turro, N., Krantz, D., Edwards, R. H., Greene, L. A., and Zecca, L. (2000) *Proc. Natl. Acad. Sci. U. S. A.* **97,** 11869–11874
20. Zecca, L., Zucca, F. A., Wilms, H., and Sulzer, D. (2003) *Trends Neurosci.* **26,** 578–580
21. Fedorow, H., Tribl, F., Halliday, G., Gerlach, M., Riederer, P., and Double, K. L. (2005) *Prog. Neurobiol.* (*Oxf.*) **75,** 109–124
22. Raper, H. S. (1928) *Physiol. Rev.* **8,** 245–282
23. Mason, H. S. (1948) *J. Biol. Chem.* **172,** 83–99
24. Greggio, E., Bergantino, E., Carter, D., Ahmad, R., Costin, G. E., Hearing, V. J., Clarimon, J., Singleton, A., Eerola, J., Hellstrom, O., Tienari, P. J., Miller, D. W., Beilina, A., Bubacco, L., and Cookson, M. R. (2005) *J. Neurochem.* **93,** 246–256
25. Garcia-Carmona, F., Garcia-Canovas, F., Iborra, J. L., and Lozano, J. A. (1982) *Biochim. Biophys. Acta.* **717,** 124–131
26. Chedekel, M. R., Land, E. J., Thompson, A., and Truscott, T. G. (1984) *J. Chem. Soc. Chem. Commun.* 1170–1172
27. Land, E. J., Ito, S., Wakamatsu, K., and Riley, P. A. (2003) *Pig. Cell Res.* **16,** 487–493
28. Palumbo, A., d'Ischia, M., Misuraca, G., and Prota, G. (1987) *Biochim. Biophys. Acta* **925,** 203–209
29. Tse, D. C. S., McCreery, R. L., and Adams, R. N. (1976) *J. Med. Chem.* **19,** 37–40
30. Bindoli, A., Rigobello, M. P., and Galzigna, L. (1989) *Toxicol. Lett.* **48,** 3–20
31. Asanuma, M., Miyazaki, I., and Ogawa, N. (2003) *Neurotox. Res.* **5,** 165–176

32. Zoccarato, F., Toscano, P., and Alexandre, A. (2005) *J. Biol. Chem.* **280,** 15587–15594
33. Hurd, R. E. (1990) *J. Magn. Res.* **87,** 422–428
34. Ancian, B., Bourgeois, I., Dauphin, J. F., and Shaw, A. A. (1997) *J. Magn. Res. A.* **125,** 348–354
35. Bax, A., and Davis, D. G. (1985) *J. Magn. Res.* **65,** 355–360
36. Griesinger, C., Otting, G., Wütrich, K., and Ernst, R. R. (1988) *J. Am. Chem. Soc.* **110,** 7870–7872
37. Pons, J. L., Malliavin, T. E., and Delsuc, M. (1996) *J. Biomol. NMR* **8,** 445–452
38. Silverstein, R. M., and Webster, F. X. (1997) *Spectrometric Identification of Organic Compounds*, 6th Ed., pp. 144–216, John Wiley & Sons, Inc.
39. Xu, R., Huang, X., Kramer, K. J., and Hawley, M. D. (1996) *Bioorg. Chem.* **24,** 110–126
40. Miller, G. W., Gainetdinov, R. R., Levey, A. I., and Caron, M. G. (1999) *Trends Pharmacol. Sci.* **20,** 424–429
41. Armarego, W. L., and Waring, P. (1983) *Biochem. Biophys. Res. Commun.* **113,** 895–899
42. Waring, P. (1986) *Eur. J. Biochem.* **155,** 305–310
43. Graham, D. G., and Jeffs, P. W. (1977) *J. Biol. Chem.* **252,** 5729–5734
44. Li, J., Zhu, M., Manning-Bog, A. B., Di Monte, D. A., and Fink, A. L., (2004) *FASEB J.* **18,** 962–964
45. Norris, E. H., Giasson, B. I., Hodara, R., Xu, S., Trojanowski, J. Q., Ischiropoulos, H., and Lee, V. M. (2005) *J. Biol. Chem.* **280,** 21212–21219
46. Aime, S., Bergamasco, B., Casu, M., Digilio, G., Fasano, M., Giraudo, S., and Lopiano, L. (2000) *Movement Disorders* **15,** 977–981